Helmholtz-Zentrum Dresden-Rossendorf (HZDR)

Development and radiosynthesis of the first 18F-labeled inhibitor of monocarboxylate transporters (MCTs)

Sadeghzadeh, M.; Moldovan, R.-P.; Fischer, S.; Wenzel, B.; Ludwig, F.-A.; Teodoro, R.; Deuther-Conrad, W.; Jonnalagadda, S.; K. Jonnalagadda, S.; Gudelis, E.; Šačkus, A.; R. Mereddy, V.; R. Drewes, L.; Brust, P.;

Perma-Link to Publication Repository of HZDR:

https://www.hzdr.de/publications/Publ-28825

Development and radiosynthesis of the first ^{18}F-labeled inhibitor of monocarboxylate transporters (MCTs)

Masoud Sadeghzadeh[1,*], Rareş-Petru Moldovan[1], Steffen Fischer[1], Barbara Wenzel[1], Friedrich-Alexander Ludwig[1], Rodrigo Teodoro[1], Winnie Deuther-Conrad[1], Shirisha Jonnalagadda[2], Sravan K. Jonnalagadda[2], Emilis Gudelis[3], Algirdas Šačkus[3], Venkatram R. Mereddy[2], Lester R. Drewes[4], Peter Brust[1]

[1]*Helmholtz-Zentrum Dresden-Rossendorf, Institute of Radiopharmaceutical Cancer Research, Department of Neuroradiopharmaceuticals, Research Site Leipzig, Permoserstraße 15, D-04318 Leipzig, Germany*

[2]*Department of Chemistry and Biochemistry, Department of Pharmacy Practice & Pharmaceutical Sciences, University of Minnesota, Duluth, MN 55812, USA*

[3]*Institute of Synthetic Chemistry, Kaunas University of Technology, K. Baršausko str. 59, Kaunas LT-51423, Lithuania*

[4]*Department of Biomedical Sciences, University of Minnesota Medical School Duluth, 251 SMed, 1035 University Drive, Duluth, MN 55812, USA*

---

[*]Corresponding author: Helmholtz-Zentrum Dresden-Rossendorf, Institute of Radiopharmaceutical Cancer Research, Department of Neuroradiopharmaceuticals, Research Site Leipzig, Permoserstraße 15, D-04318 Leipzig, Germany, E-mail address: m.sadeghzadeh@hzdr.de (Masoud Sadeghzadeh), Tel: +49 351 260 4630

Abstract

Monocarboxylate transporters 1 and 4 (MCT1 and MCT4) are involved in tumor development and progression. Their expression levels are related to clinical disease prognosis. Accordingly, both MCTs are promising drug targets for treatment of a variety of human cancers. The non-invasive imaging of these MCTs in cancers is regarded to be advantageous for assessing MCT-mediated effects on chemotherapy and radiosensitization using specific MCT inhibitors. Herein, we describe a method for the radiosynthesis of [^{18}F]**FACH** (*(E)*-2-cyano-3-{4-[(3-[^{18}F]fluoropropyl)(propyl) amino]-2-methoxyphenyl}acrylic acid), as a novel radiolabeled MCT1/4 inhibitor for imaging with PET. A fluorinated analog of α-cyano-4-hydroxycinnamic acid (**FACH**) was synthesized and the inhibition of MCT1 and MCT4 was measured via an [^{14}C]lactate uptake assay. Radiolabeling was performed via a two-step protocol comprising the radiosynthesis of the intermediate *(E)/(Z)*-[^{18}F]***tert*-Bu-FACH** (*tert*-butyl *(E)/(Z)*-2-cyano-3-{4-[(3-[^{18}F]fluoropropyl)(propyl)amino]-2-methoxyphenyl}acrylate) followed by deprotection of the *tert*-butyl group. The radiofluorination was successfully implemented using either K[^{18}F]F-K$_{2.2.2}$-carbonate or [^{18}F]TBAF. The final deprotected product [^{18}F]**FACH** was only obtained when [^{18}F]***tert*-Bu-FACH** was formed by the latter procedure. After optimization of the deprotection reaction, [^{18}F]**FACH** was obtained in high radiochemical yields (39.6 ± 8.3%, EOB) and radiochemical purity (>98%).

Keywords: Radiofluorination, [^{18}F]**FACH**, Positron emission tomography (PET), Monocarboxylate transporters (MCTs), α-cyano-4-hydroxycinnamic acid (α-CHC)

1 INTRODUCTION

Monocarboxylate transporters (MCTs) belong to the solute carrier 16 (SLC16) gene family and comprise of 14 isoforms, each having a unique distribution and different sequence homology (1). Among them, MCT1 and MCT4 act as H^+-linked transporters of short-chain monocarboxylates (e.g. pyruvate, L-lactate, and ketone bodies) across the plasma membrane of mammalian cells (2-4). They have also shown to play an important role in supporting the lactate oxidation pathway and facilitating metabolic symbiosis (5). Cancer cells avoid cytoplasmic acidification that may lead to apoptosis by facilitated efflux of pyruvate and lactate produced during glycolysis (5, 6). Accordingly, upregulation of MCTs, in particular of MCT1 and MCT4, has been observed in a large number of tumors (7-13). Consequently, these two isoforms are known as major selective targets for the treatment of a broad spectrum of cancers such as high-grade gliomas, neuroblastomas, soft tissue sarcoma, colorectal carcinomas, lung cancer, cervical cancer and triple-negative breast carcinoma (7-13). It has been shown that inhibition of MCT1 and/or MCT4 can block tumor growth through disruption of lactate transport and the glycolytic pathway of cell energy metabolism (14).

The development and preclinical evaluation of several MCT inhibitors including α-cyanocinnamate derivatives, quinolinethiophene amides such as AZD3965 and AR-C155858 as well as bioflavenoids such as quercetin, phenyl pyruvate, and phloretin (Figure 1A) have been reported (1, 15-17). Among these drugs, AZD3965, initially developed as an immunosuppressor (17), is currently being evaluated as an anticancer agent in Phase I clinical trials (NCT01791595) for patients with prostate cancer, gastric cancer or diffuse large B cell lymphoma (18). Although having relatively low inhibitory activity towards MCT1 ($IC_{50} \sim 100$ μM), α-cyano-4-hydroxycinnamic acid (α-CHC) was the first MCT1 inhibitor reported (19). More recently, we reported a comprehensive structure-activity relationship (SAR) study on a new series of α-CHC derivatives as MCT1 inhibitors (7, 8). Accordingly, we have also described the synthesis of the most potent inhibitors in this series and reported on their *in vivo* tumor growth inhibition in WiDr tumor-bearing mice for potential anticancer applications (7, 8).

In this context, it is also of high interest to attain a more detailed understanding of the function and regulation of MCTs in living animals and humans by positron emission tomography (PET). From the diagnostic perspective, the involvement of MCT1 and MCT4 in the glycolytic metabolism of cancer cells makes them valuable imaging biomarkers for many tumors. However, during the last decade only a few substrates and inhibitors of MCTs were investigated as PET tracers (Figure 1B) for *in vivo* investigation of MCTs (20-22).

We have focused on α-CHC derivatives as lead compounds to develop a novel ^{18}F-labeled ligand targeting MCTs for tumor imaging with PET. To achieve this aim, *(E)*-2-cyano-3-(4-(dipropylamino)-2-methoxyphenyl)acrylic acid **(I)** (Figure 2) appeared to be appropriate because it shows a high MCT1 inhibition ($IC_{50} = 12 \pm 1$ nM) (7, 8). Based on **I**, a fluorinated derivative namely, **FACH** (*(E)*-2-cyano-3-{4-[(3- fluoropropyl)(propyl)amino]-2-methoxyphenyl} acrylic
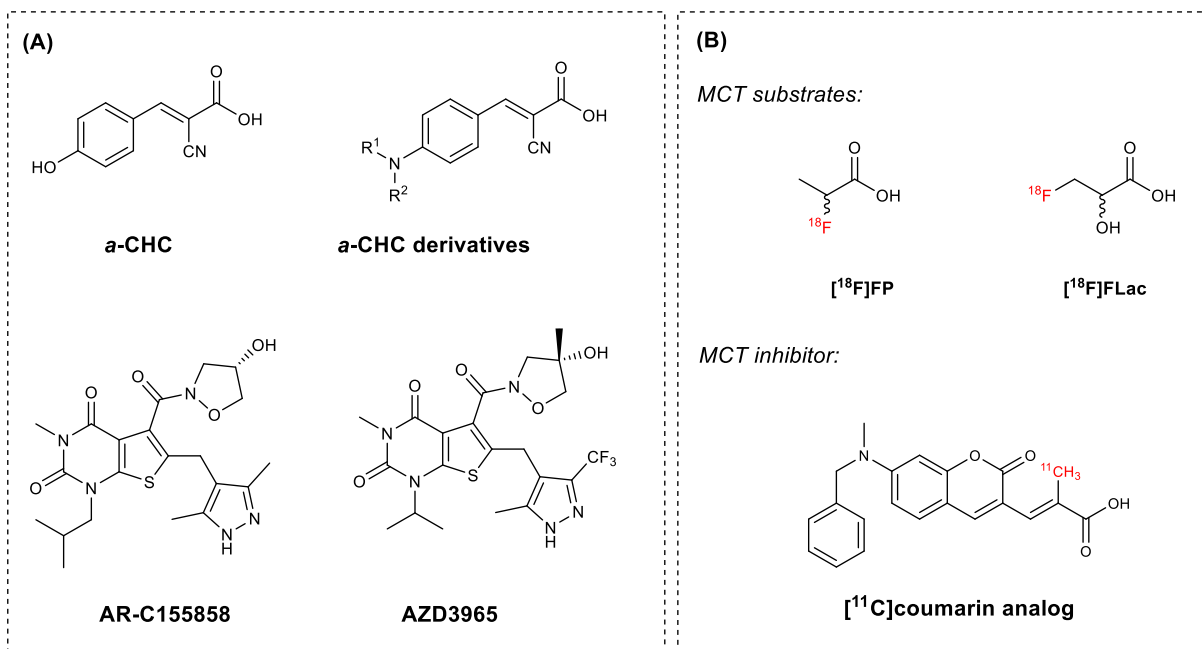
FIGURE 1 (A) Selected potent MCTs inhibitors; (B) Recently developed [18]F- and ^{11}C-labeled MCT-targeting tracers (15-22)

acid), has been developed in the present study and considered as a candidate for ^{18}F-labeling (Figure 2). Herein, we report on the chemical synthesis, measurement of MCT inhibition and radiosynthesis of the first ^{18}F-labeled MCTs inhibitor [^{18}F]**FACH**.
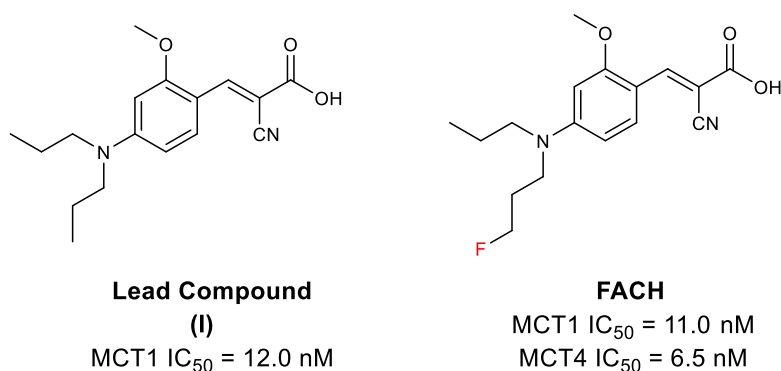
FIGURE 2 The potent MCT1 inhibitor (**I**) and its fluorinated analog (**FACH**) developed in the present study

2 MATERIALS AND METHODS

2.1 Organic syntheses

2.1.1 General methods

4

Unless otherwise noted, moisture-sensitive reactions were conducted under dry nitrogen or argon. All chemicals and reagents were purchased from commercial sources and used without further purification. Thin layer chromatography (TLC): Silica gel 60 F254 plates (Merck KGaA, Darmstadt, Germany). Flash chromatography (fc): Silica gel 60, 40-64 μm (Merck). Room temperature was 21 °C. MS: MAT GCQ (Thermo Finnigan MAT GmbH, Bremen, Germany). ^{1}H and ^{13}C spectra were recorded on VARIAN "MERCURY plus" (300 MHz for ^{1}H NMR, 75 MHz for ^{13}C NMR) and VARIAN "MERCURY plus" and BRUKER DRX-400 (400 MHz for ^{1}H NMR, 100 MHz for ^{13}C NMR, 377 MHz); δ in ppm related to tetramethylsilane; coupling constants (J) are given with 0.1 Hz resolution. Multiplicities of NMR signals are indicated as follows: s (singlet), d (doublet), t (triplet), m (multiplet), dd (doublet of doublets), dt (doublet of triplets). ESI/Ion trap mass spectra (LRMS) were recorded with a Bruker Esquire 3000 plus instrument (Billerica, MA, USA). High resolution mass spectra were recorded on a FT-ICR APEX II spectrometer (Bruker Daltonics; Bruker Corporation, Billerica, MA, USA) using electrospray ionization (ESI) in positive ion mode.

2.1.2 General procedure for synthesis of the reference compounds and precursor

1-Bromopropane (2.55 mL, 28 mmol, 1.0 eq) and potassium carbonate (8.4 g, 60 mmol, 2.1 eq) were added to a solution of *m*-anisidine (6.0 mL, 84 mmol, 3 eq) in 50 mL acetonitrile (ACN) and refluxed overnight. Upon the completion of the reaction, 100 mL 5% aqueous $NaHCO_3$ solution was added and the mixture was extracted with ethyl acetate (EtOAc, 3×50 mL). The organic layer was dried with anhydrous Mg_2SO_4 and evaporated. The residue was purified by column chromatography (silica, EtOAc/isohexane (IH) = 0.5:9.5 to 1:9) to give the monoalkylated aniline [52% yield, TLC (silica gel, EtOAc/IH, 2:8): R_f = 0.65]. 1-Iodo-3-fluoropropane (2.65 mL, 20 mmol, 1.8 eq) and potassium carbonate (4.2 g, 30 mmol, 2.7 eq) were added to a solution of 3-methoxy-*N*-propylaniline (1.82 g, 11 mmol, 1.0 eq) in 50 mL ACN and refluxed overnight. Upon the completion of the reaction, 100 mL 5% aqueous $NaHCO_3$ solution was added and the mixture was extracted with EtOAc (3×50 mL). The organic layer was dried with anhydrous Mg_2SO_4 and evaporated. $POCl_3$ (1.0 mL, 11 mmol, 1.1 eq) was added dropwise to a solution of dialkylated aniline (10 mmol, 1.0 eq) in dimethylformamide (DMF, 4.65 mL, 60 mmol, 6.0 eq) at 0 °C and the reaction mixture was refluxed at 80 °C for 2-4 hours. The reaction was quenched with saturated Na_2CO_3 and the solid was filtered and washed with n-hexane to obtain the corresponding *N,N*-disubstituted benzaldehyde. Cyanoacetic acid (or *t*-butyl cyanoacetate) (15 mmol, 3.0 eq) and piperidine (0.5 mL, 5 mmol, 1.0 eq) were added to a solution of substituted benzaldehyde (5 mmol, 1.0 eq) in 20 mL ACN and refluxed overnight at 80 °C. Upon the completion of the reaction, the above solution was poured into a mixture of 3M HCl (10 mL) in ice. The solution was stirred for 10 to 15 minutes and the solid was filtered using a Büchner funnel. The final compounds were obtained in pure form by column chromatography.

N-(3-Fluoropropyl)-3-methoxy-*N*-propylaniline (**2**) (colorless oil, 96% yield). TLC (silica gel, EtOAc/IH, 2:8): R_f = 0.82. ^{1}H NMR (400 MHz, DMSO-d_6) δ 7.13 (t, J = 8.6 Hz, 1H), 6.45–6.06

(m, 3H), 4.57 (t, $J = 5.6$ Hz, 1H), 4.45 (t, $J = 5.6$ Hz, 1H), 3.79 (s, 3H), 3.45 (t, $J = 7.1$ Hz, 2H), 3.23 (m, 2H), 2.30–1.80 (m, 2H), 1.69 (q, $J = 7.6$ Hz, 2H), 0.99 (t, $J = 7.4$ Hz, 3H).

4-[(3-Fluoropropyl)(propyl)amino]-2-methoxybenzaldehyde (**3**) (yellow solid, >98% yield). TLC (silica gel, EtOAc/IH, 2:8): $R_f = 0.18$. [^1]H NMR (400 MHz, chloroform-d) δ 10.15 (s, 1H), 7.71 (d, $J = 8.9$ Hz, 1H), 6.30 (dd, $J = 8.9, 2.3$ Hz, 1H), 6.12 (d, $J = 2.4$ Hz, 1H), 4.61 (t, $J = 5.4$ Hz, 1H), 4.49 (t, $J = 5.4$ Hz, 1H), 3.90 (s, 3H), 3.58 (t, $J = 7.2$ Hz, 2H), 3.35 (dd, $J = 9.1, 6.3$ Hz, 2H), 2.34–1.88 (m, 2H), 1.69 (q, $J = 7.6$ Hz, 2H), 0.99 (t, $J = 7.4$ Hz, 3H); [^13]C NMR (100 MHz, chloroform-d) δ 187.2, 164.0, 154.1, 130.7, 114.6, 104.4, 92.9, 81.4 (d, $J = 164.9$ Hz), 55.2, 52.8, 47.0 (d, $J = 3.5$ Hz), 28.4 (d, $J = 20.1$ Hz), 20.5, 11.3.

(*E*)-2-Cyano-3-{4-[(3-fluoropropyl)(propyl)amino]-2-methoxyphenyl}acrylic acid (**FACH**) (yellow solid, 90% yield). TLC (silica gel, EtOAc/IH, 1:1): $R_f = 0.33$. [^1]H NMR (400 MHz, DMSO-d_6) δ 8.40 (s, 1H), 8.18 (d, $J = 9.2$ Hz, 1H), 6.50 (dd, $J = 9.3, 2.4$ Hz, 1H), 6.19 (d, $J = 2.4$ Hz, 1H), 4.57 (t, $J = 5.7$ Hz, 1H), 4.45 (t, $J = 5.6$ Hz, 1H), 3.86 (s, 3H), 3.67–3.46 (m, 2H), 3.38 (t, $J = 7.6$ Hz, 2H), 2.06–1.79 (m, 2H), 1.58 (h, $J = 7.4$ Hz, 2H), 0.89 (t, $J = 7.4$ Hz, 3H); [^13]C NMR (100 MHz, DMSO-d_6) δ 165.8, 162.1, 154.5, 146.7, 130.3, 118.9, 108.2, 105.9, 93.8, 91.6, 82.2 (d, $J = 161.4$ Hz), 56.1, 52.2, 46.9 (d, $J = 4.8$ Hz), 28.4 (d, $J = 19.3$ Hz), 20.6, 11.5. HRFT-MS (ESI+): $m/z = 343.1422$ (calcd. 343.1428 for $C_{17}H_{21}FN_2O_3Na^+$ [M+Na]$^+$).

tert-Butyl *(E)/(Z)*-2-cyano-3-{4-[(3-fluoropropyl)(propyl)amino]-2-methoxyphenyl}acrylate (**(E)/(Z)-*tert*-Bu-FACH**) (yellow solid, >98% yield). TLC (silica gel, EtOAc/IH, 1:1): $R_f = 0.50$. [^1]H NMR (400 MHz, chloroform-d) δ 8.56 (s, 1H), 8.36 (d, $J = 9.0$ Hz, 1H), 6.33 (dd, $J = 9.2, 2.5$ Hz, 1H), 6.09 (d, $J = 2.5$ Hz, 1H), 4.58 (t, $J = 5.4$ Hz, 1H), 4.46 (t, $J = 5.4$ Hz, 1H), 3.84 (s, 3H), 3.65–3.48 (m, 2H), 3.42–3.27 (m, 3H), 2.12–1.86 (m, 2H), 1.65 (td, $J = 15.6, 8.0$ Hz, 2H), 1.55 (s, 9H), 1.03–0.88 (m, 3H); [^13]C NMR (100 MHz, chloroform-d) δ 163.7, 161.9, 153.6, 147.2, 131.1, 118.4, 109.5, 105.0, 94.2, 93.0 (d, $J = 1.1$ Hz), 84.3, 82.0, 80.4, 55.3, 52.9, 47.0 (d, $J = 3.5$ Hz), 28.5 (d, $J = 20.0$ Hz), 28.1, 25.9, 20.6, 11.3. HRFT-MS (ESI+): $m/z = 377.2233$ (calcd. 377.2235 for $C_{21}H_{30}FN_2O_3$ [M+H]$^+$).

3-[(3-Methoxyphenyl)(propyl)amino]propan-1-ol (**5**). 3-Bromo-1-propanol (1.81 mL, 20 mmol, 1.8 eq) and potassium carbonate (4.2 g, 30 mmol, 2.7 eq) were added to a solution of 3-methoxy-*N*-propylaniline (1.82 g, 11 mmol, 1.0 eq) in 50 mL ACN and refluxed overnight. The work-up was performed as described in the general procedure (yellow oil, 88% yield). TLC (silica gel, EtOAc/IH, 2:8): $R_f = 0.19$. [^1]H NMR (400 MHz, chloroform-d) δ 7.15 (t, $J = 8.1$ Hz, 1H), 6.38 (dd, $J = 8.4, 2.4$ Hz, 1H), 6.34–6.10 (m, 2H), 3.82 (s, 3H), 3.74 (t, $J = 6.0$ Hz, 2H), 3.44 (t, $J = 7.1$ Hz, 2H), 3.34–3.16 (m, 2H), 2.03 (s, 1H), 1.91–1.76 (m, 2H), 1.64 (h, $J = 7.4$ Hz, 2H), 0.95 (t, $J = 7.4$ Hz, 3H); [^13]C NMR (100 MHz, chloroform-d) δ 160.9, 149.6, 129.9, 105.8, 100.6, 99.3, 60.8, 55.1, 53.3, 48.1, 30.2, 20.3, 11.5.

3-[(3-Methoxyphenyl)(propyl)amino]propyl acetate (**6**). Acetyl chloride (2.4 mL, 33 mmol, 1.5 eq) and pyridine (5.3 mL, 66 mmol, 3.0 eq) was added to a solution of alcohol **5** (5.0 g, 22 mmol,

1.0 eq) in 50 mL dichloromethane (DCM) and the resulting mixture was allowed to react at room temperature overnight. The reaction was quenched by the addition of 50 mL ice cold water, the phases were separated and the organic phase was dried with anhydrous Mg_2SO_4 and evaporated to give **6** as yellowish oil which was used in the next reaction without further purification. TLC (silica gel, EtOAc/IH, 2:8): $R_f = 0.55$. ^1H NMR (400 MHz, chloroform-*d*) δ 7.14 (t, *J* = 8.1 Hz, 1H), 6.46–6.07 (m, 3H), 4.14 (t, *J* = 6.3 Hz, 2H), 3.81 (s, 3H), 3.39 (t, *J* = 7.3 Hz, 2H), 3.24 (t, *J* = 7.7 Hz, 2H), 2.10 (s, 3H), 1.95 (t, *J* = 7.1 Hz, 2H), 1.63 (m, 2H), 0.94 (t, *J* = 7.4 Hz, 3H); ^{13}C NMR (100 MHz, chloroform-*d*) δ 171.1, 160.9, 149.3, 129.9, 105.3, 100.3, 98.8, 62.4, 55.1, 53.1, 47.8, 26.6, 21.0, 20.4, 11.4.

3-[(4-Formyl-3-methoxyphenyl)(propyl)amino]propyl acetate (**7**) (yellow oil, 79% yield). TLC (silica gel, EtOAc/IH, 2:8): $R_f = 0.11$. ^1H NMR (400 MHz, chloroform-*d*) δ 10.19 (s, 1H), 7.76 (d, *J* = 8.9 Hz, 1H), 6.39 (dd, *J* = 8.9, 2.3 Hz, 1H), 6.29 (s, 1H), 4.16 (t, *J* = 6.2 Hz, 2H), 3.93 (s, 3H), 3.57–3.42 (m, 2H), 3.42–3.25 (m, 2H), 2.10 (s, 3H), 2.01 (m, 2H), 1.71 (m, 2H), 0.99 (t, *J* = 7.4 Hz, 3H).

4-[(3-Hydroxypropyl)(propyl)amino]-2-methoxybenzaldehyde (**8**). A solution of K_2CO_3 (7.0 g, 50 mmol, 5.0 eq) in 70 mL H_2O was added to a solution of **7** (2.5 g, 10 mmol, 1.0 eq) in 75 mL MeOH and the reaction mixture was stirred for 30 min at room temperature. An aqueous saturated NaCl solution (50 mL) was added, followed by addition of 100 mL DCM. The resulting phases were separated and the organic phase was dried with anhydrous Mg_2SO_4 and evaporated to give **8** as yellowish oil which was used in the next reaction without further purification. TLC (silica gel, EtOAc/IH, 1:1): $R_f = 0.15$. ^1H NMR (400 MHz, chloroform-*d*) δ 10.16 (s, 1H), 7.73 (d, *J* = 8.9 Hz, 1H), 6.38 (d, *J* = 9.0 Hz, 1H), 6.28 (s, 1H), 3.91 (s, 3H), 3.76 (t, *J* = 5.8 Hz, 2H), 3.57 (t, *J* = 7.3 Hz, 2H), 3.36 (dd, *J* = 8.6, 6.9 Hz, 2H), 1.97–1.84 (m, 2H), 1.70 (h, *J* = 7.5 Hz, 2H), 0.98 (t, *J* = 7.4 Hz, 3H).

tert-Butyl *(E)/(Z)*-2-cyano-3-{4-[(3-hydroxypropyl)(propyl)amino]-2-methoxyphenyl}acrylate (**9**) (yellow solid, 90%). TLC (silica gel, EtOAc/IH, 1:1): $R_f = 0.18$. ^1H NMR (300 MHz, chloroform-*d*) δ 8.56 (s, 1H), 8.35 (d, *J* = 9.2 Hz, 1H), 6.38 (dd, *J* = 9.1, 2.4 Hz, 1H), 6.20 (s, 1H), 3.85 (s, 3H), 3.73 (t, *J* = 5.8 Hz, 2H), 3.55 (dd, *J* = 8.1, 6.4 Hz, 2H), 3.38–3.28 (m, 2H), 1.92–1.84 (m, 2H), 1.67 (dt, *J* = 9.4, 7.4 Hz, 2H), 1.57 (s, 9H), 0.95 (t, *J* = 7.4 Hz, 3H). ^{13}C NMR (75 MHz, chloroform-*d*) δ 165.5, 162.3, 154.3, 148.1, 131.2, 118.6, 109.2, 105.3, 93.1, 91.0, 59.7, 55.4, 52.8, 52.6, 47.8, 30.1, 20.6, 14.2, 11.4. HRFT-MS (ESI+): *m/z* = 375.2340 (calcd. 375.2278 for $C_{21}H_{31}N_2O_4^+$ [M+H]$^+$).

tert-Butyl *(E)/(Z)*-2-cyano-3-{2-methoxy-4-{[3-[(methylsulfonyl)oxy]propyl](propyl)amino} phenyl}acrylate (**10**). Methanesulfonyl chloride (30 µL, 0.4 mmol, 1.2 eq) and triethylamine (Et₃N, 130 µL, 0.9 mmol, 3.0 eq) were added to a solution of alcohol **9** (100 mg, 0.3 mmol, 1.0 eq) in 5 mL DCM and the reaction mixture was stirred for 30 minutes at room temperature. The reaction was quenched by addition of 10 mL saturated aqueous NaHCO₃ solution. The aqueous solution was extracted with DCM (2 × 10 mL) and the combined organic phases were washed with

brine (10 mL) and dried over MgSO$_4$. Evaporation of the solvent under reduced pressure afforded quantitatively the corresponding mesylate **10** as yellow solid with >98% yield. TLC (silica gel, EtOAc/IH, 1:1): R_f = 0.22. ^{1}H NMR (400 MHz, chloroform-*d*) δ 8.57 (t, *J* = 0.5 Hz, 1H), 8.36 (dd, *J* = 9.2, 0.5 Hz, 1H), 6.32 (dd, *J* = 9.2, 2.4 Hz, 1H), 6.07 (d, *J* = 2.5 Hz, 1H), 4.30 (t, *J* = 5.8 Hz, 2H), 3.85 (s, 3H), 3.64–3.48 (m, 2H), 3.42–3.26 (m, 2H), 3.03 (s, 3H), 2.15–2.01 (m, 2H), 1.67 (q, *J* = 7.6 Hz, 2H), 1.55 (s, 9H), 0.96 (t, *J* = 7.4 Hz, 3H). ^{13}C NMR (100 MHz, chloroform-*d*) δ 163.6, 161.9, 153.3, 147.2, 131.1, 118.40, 109.67, 105.03, 94.59, 93.15, 82.15, 67.35, 55.46, 52.98, 47.22, 37.45, 28.10, 27.20, 20.60, 11.4. HRFT-MS (ESI+): *m/z* = 453.2134 (calcd. 453.2054 for C$_{22}$H$_{33}$N$_2$O$_6$S$^+$ [M+H]$^+$).

2.2 [^{14}C]Lactate uptake assay for assessment of MCT1 and MCT4 inhibition

Inhibition of MCT1-mediated lactate transport was determined in rat brain endothelial cell line (RBE4) as previously described (7, 8). PCR analysis and Western Blot demonstrated that only the MCT1 isoform is expressed by RBE4 cells (data not shown). For determination of the inhibition of MCT4-mediated transport, MB-231 cells were used because these cells express exclusively MCT4 as determined by PCR and Western Blot (data not shown). For both cell lines, an L-[^{14}C]lactate based transport assay was implemented to quantify the transport of lactate via the respective MCT and the inhibition thereof by **FACH**. Cells were seeded at 4×10^5 cells/mL in 24-well culture dishes. After 24 hours, cells were washed twice with 500 µL HEPES buffer and allowed to equilibrate for 15-20 minutes at 37 °C. Afterwards, cells were incubated for one hour in the presence of L-[^{14}C]lactate and different concentrations (100 pM – 1 µM) of the respective test compound. The DMSO stock solution of **FACH** was diluted to the respective working concentration in HEPES buffer (140 mM NaCl, 5 mM KCl, 2 mM CaCl$_2$, 2 mM MgCl$_2$, 10 mM HEPES, pH 7.0) containing 3 µM L-[^{14}C]lactate (Perkin Elmer) and 2 µM L-lactate. α-CHC and dimethylsulfoxide (DMSO) were used as positive and vehicle controls. The incubation was terminated by replacing the incubation medium with 500 µL ice-cold HEPES buffer (containing 0.1 mM α-CHC, pH 7.4) and transferring the plates on ice. Cells were washed twice with ice-cold HEPES buffer and finally solubilized using 250 µL of 0.1 M NaOH in 5% Triton-X (Millipore Sigma). A 150 µL aliquot from each well was added to 4 mL EcoLite(+)^{TM} scintillation fluid (MP Biomedicals) and radioactivity was determined by scintillation spectrometry. The inhibition of L-[^{14}C]lactate uptake by each test solution was calculated as a percentage of the maximum control uptake and IC$_{50}$ values were calculated using GraphPad PRISM.

2.3 Radiochemistry

2.3.1 General methods

A Nirta XL target filled with [^{18}O]H$_2$O (Hyox 18 enriched water, Rotem Industries Ltd., Arava, Israel) attached to the Cyclone 18/9 (iba RadioPharma Solutions, Belgium) was irradiated with fixed energy proton beam to produce no-carrier-added [^{18}F]fluoride via the [^{18}O(p,n)^{18}F] nuclear reaction. Discover PET Wave Microwave (CEM, NC, USA) was used for the azeotropic drying

process of [^{18}F]fluoride. Radio thin-layer chromatography (radio-TLC) analyses were carried out on silica gel (Polygram SIL G/UV254) and aluminum oxide (Polygram Alox N/UV254) pre-coated plates developed with EtOAc/n-hexane 1:1 (for [^{18}F]***tert*-Bu-FACH**) and DCM/MeOH 8:2 (for [^{18}F]**FACH**), respectively. The plates were exposed to storage phosphor screens (BAS-MS2025, FUJIFILM Co., Tokyo, Japan) and recorded using the Amersham Typhoon RGB Biomolecular Imager (GE Healthcare Life Sciences). Images were quantified with the Image Quant TL8.1 software (GE Healthcare Life Sciences).

Analytical chromatographic separations were performed on a JASCO LC-2000 system (JASCO Labor- und Datentechnik, Gross-Umstadt, Germany), incorporating a PU-2080 Plus pump, AS-2055 Plus auto injector (100 μL sample loop), and a UV-2070 Plus detector coupled with a gamma radioactivity HPLC detector (Gabi Star, Raytest Isotopenmessgeräte GmbH, Straubenhardt, Germany). Data analysis was performed with the Galaxie chromatography software (Agilent Technologies) using the chromatograms obtained at 210 and 254 nm. Semi-preparative HPLC separations were performed on a JASCO LC-2000 system, including a PU-2080-20 pump, a UV/vis-2075 detector coupled with a gamma radioactivity HPLC detector with slightly modified measurement geometry (Gabi Star, Raytest Isotopenmessgeräte GmbH), and a fraction collector (Advantec CHF- 122SC, Dublin, CA, USA). Data analysis was performed with the Galaxie chromatography software (Agilent Technologies) using the chromatograms obtained at 254 nm. The ammonium acetate (NH$_4$OAc) and ammonium formate (NH$_4$HCO$_2$) concentrations (20 mM NH$_4$OAc/NH$_4$HCO$_2$ aq.) correspond to the concentrations in the aqueous component of an eluent mixture.

2.3.2 General procedure for radiosynthesis of [^{18}F]FACH by using K[^{18}F]F-K$_{2.2.2}$-carbonate complex

No-carrier-added [^{18}F]fluoride (1-2 GBq) in 1 mL of H$_2$O was trapped on a Chromafix 30 PS-HCO$_3$-cartridge (Macherey-Nagel GmbH & Co. KG, Düren, Germany). The activity was eluted with 300 μL of an aqueous solution of potassium carbonate (K$_2$CO$_3$, 1.5 mg, 10.5 μmol) into a 4 mL V-shape vial containing Kryptofix 2.2.2 (K$_{2.2.2}$, 11.2 mg, 29.5 μmol) in 1 mL of ACN. The aqueous [^{18}F]fluoride was azeotropically dried under *vacuum* and nitrogen flow within 7-10 min using a single mode microwave device (75 W, at 50-60 °C, power cycling mode). Two times 1.0 mL of ACN were added during the drying procedure, and the final complex was dissolved in 500 μL of ACN or DMSO. Thereafter, certain volumes of the K[^{18}F]F-K$_{2.2.2}$-carbonate complex, which correspond to the required amount of the complex, was added to a solution of 2 mg of precursor **10** in 500 μL of ACN or DMSO. Radiofluorination was performed under conventional heating at different temperatures in a total volume of 750 μL. To determine the radiochemical yields of the products by radio-HPLC and radio-TLC, samples were taken from each crude reaction mixture at different time points after cooling the vial in ice to < 30 °C.

After cooling the vial to room temperature, HCl (2.0 and 6.0 N) or TFA was added to the crude mixture and the deprotection reaction was performed during different reaction times at different

temperatures. Thereafter, aqueous 2.0 M NaOH or saturated Na_2CO_3 was used for neutralization of the reaction mixture. In case of performing the deprotection in dichloromethane (DCM), the evaporation of ACN and re-dissolving the residue in 100 μL of dry DCM was needed. Evaporation of remaining TFA was considered as an alternative for neutralization when ACN or DCM were used as solvent. In this case, volatile solvents were evaporated at room temperature under *vacuum* and a gentle stream of argon.

2.3.3 General procedure for radiosynthesis of [^{18}F]FACH by using [^{18}F]TBAF

The aqueous solution of no-carrier-added [^{18}F]fluoride was added to a solution of 50 μL of tetra-n-butylammonium bicarbonate (0.075 M) in 1 mL of ACN to a V-shape reaction vial. The aqueous [^{18}F]fluoride was azeotropically dried under *vacuum* and nitrogen flow within 7-10 min using a single mode microwave device (75 W, at 50−60 °C, power cycling mode). Two times 1.0 mL of ACN were added during the drying procedure, and the final complex was dissolved in 250 μL of ACN ready for labeling. A solution of 2 mg of precursor **10** in 500 μL of *tert*-BuOH or ACN was added to the reaction vial, sealed and mixed. The mixture with a total volume of 750 μL was heated at 100 °C for up to 20 min. After completion of the reaction, the reaction mixture was allowed to cool to < 40 °C and the solvents were evaporated under *vacuum* and a gentle stream of argon at 40 °C for 6-10 min. Thereafter, 100 μL of fresh ACN was added to the residue and then 400 μL of TFA were slowly added. The deprotection was conducted at room temperature for up to 20 min. Sampling was carried out at desired time points to determine the optimized reaction time for both steps. Neutralization was performed by addition of the required amount of Et_3N to adjust the pH to 4-5 and subjected to a semi-preparative RP-HPLC for isolation of [^{18}F]**FACH** (46% ACN/20 mM NH_4HCO_2, pH = 4-5, 3.5 mL/min, Reprosil-Pur C18-AQ column, 250 mm × 10 mm; 5 μm; Dr. Maisch HPLC GmbH, Ammerbuch-Entringen, Germany). The collected radiotracer fraction was diluted with 40 mL of H_2O to perform final purification by sorption on a Sep-Pak C18 light cartridge (Waters, Milford, MA, USA) and successive elution with 0.75 mL of ethanol. The solvent was reduced under a gentle argon stream and the desired radiotracer was formulated in sterile isotonic saline containing 10% EtOH (v/v).

Identity and radiochemical purity of [^{18}F]**FACH** was confirmed by radio-HPLC (gradient and isocratic modes) and radio-TLC (SIL G/UV254, DCM/MeOH 8:2). For analytical radio-HPLC, a Reprosil-Pur C18-AQ column (250 mm × 4.6 mm; 5 μm; Dr. Maisch HPLC GmbH; Germany) and an eluent mixture containing ACN mixed with aqueous 20 mM NH_4OAc or NH_4HCO_2 was used with a flow of 1.0 mL/min (see supplementary data). Molar activity was determined based on a calibration curve carried out under isocratic HPLC conditions (46% ACN/ aq. 20 mM NH_4HCO_2, pH = 4-5) using chromatograms obtained at 210 nm.

3 RESULTS AND DISCUSSION

### 3.1 Organic chemistry and MCT inhibition

In order to develop a fluorinated analog of the lead compound **I**, we replaced one of the propyl groups attached to the amino function by a fluoropropyl group. The synthesis of compound **I** was previously described in three steps starting from *m*-anisidine in 67% overall yield (7). A similar synthetic approach was used to synthesize the new fluorinated derivative **FACH** (Scheme 1). Additionally, the carbonic acid protected derivative ***tert*-Bu-FACH** was synthesized, as this compound would necessarily be an intermediate in the ^{18}F-radiosynthesis. Briefly, *N,N*-dialkylated anisidine **2** was formed via two consequence alkylation reactions on *m*-anisidine **1** followed by a Vilsmeier-Haack formylation to give compound **3** in 49% yield (three steps) (23). The Knoevenagel condensation reaction of aldehyde **3** with cyanoacetic acid and *tert*-butyl cyanoacetate afforded **FACH** and ***tert*-Bu-FACH** in 44% and 48% overall yields, respectively (Scheme 1). The characterization of ***tert*-Bu-FACH** by HPLC and LC-MS revealed that a mixture of *E*- and *Z*-isomers was obtained whereas the *E*-isomer was the predominant product (E/Z = 96:4; Figures S2.1 and S2.2). According to the reported ^{1}H NMR data, the chemical shift for the alkene hydrogen in the *Z*-isomer could be distinguishable in coumarin analogs (22). However, in our case the characterization of *(Z)-**tert*-Bu-FACH** was not possible by NMR analyses probably due to the very low ratio of *Z*-isomer compared to the *E*-isomer (Figures S3.1 and S3.2).
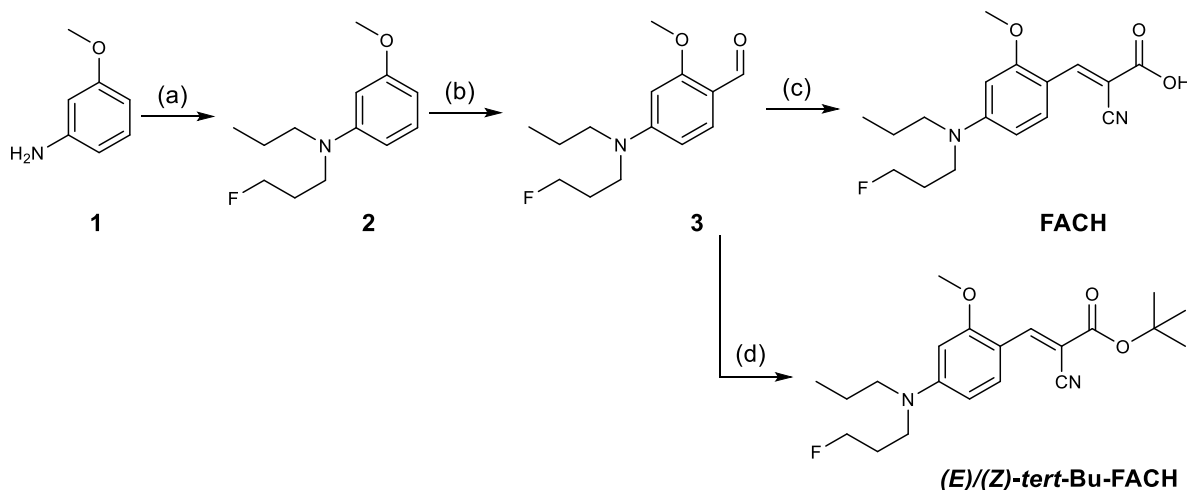
SCHEME 1 Synthesis of the reference compounds **FACH** and ***tert*-Bu-FACH**: a) *i*. Br(CH$_2$)$_3$, K$_2$CO$_3$, ACN, reflux, overnight, 52%; *ii*. I(CH$_2$)$_3$F, K$_2$CO$_3$, ACN, reflux, 96%; b) POCl$_3$/DMF, 80 °C, 98%; c) cyanoacetic acid, piperidine, ACN, reflux, 90%; d) *tert*-butyl cyanoacetate, piperidine, ACN, reflux, 98%

In order to determine the inhibitory potency of **FACH** towards MCT1 and MCT4, an L-[^{14}C]lactate uptake assay was performed using RBE4 and MDA-MB-231 cells, respectively (7, 8). **FACH** revealed high MCT1 and MCT4 inhibition (IC$_{50}$ = 11.0 nM and 6.5 nM, respectively; Figure S4.1) comparable to the corresponding lead compound **I** (Figure 2). The high MCT4 inhibition found for **FACH** is favorable for further investigations considering the high density of MCT4 in several tumors cells (e.g. brain, breast and prostate) (9-13).

For the radiosynthesis of new PET radioligand [^{18}F]**FACH**, a precursor compound with a suitable leaving group for nucleophilic aliphatic substitution with [^{18}F]fluoride is required. Furthermore, protection of the carboxylic acid group was performed to prevent its interference in the radiofluorination step. The synthesis route is depicted in Scheme 2. Starting with the treatment of 3-methoxy-*N*-propylaniline **4** with 3-bromo-1-propanol afforded 3-[(3-methoxyphenyl)(propyl) amino]propan-1-ol **5** in 88% yield. In order to avoid side reactions in the formylation step, conversion of the alcoholic group to its corresponding acetate **6** was performed. Removal of the protecting group after Vilsmeier-Haack formylation afforded the aldehyde **8** which was subjected to the Knoevenagel condensation with *tert*-butyl cyanoacetate to give the protected alcohol **9**. The mesylate precursor **10** was finally prepared by treating the alcohol **9** with methanesulfonyl chloride and trimethylamine in 62% overall yield (Scheme 2). According to the ^{1}H NMR data, a mixture of *E*- and *Z*-isomers of the mesylate precursor **10** was found. Further HPLC and LC-MS analyses revealed an approximate ratio of 4:1 for isomer *E* to *Z* (Figures S2.3 and S2.4). The chemical purity of the mesylate precursor **10** was estimated to be >95% including both isomers.
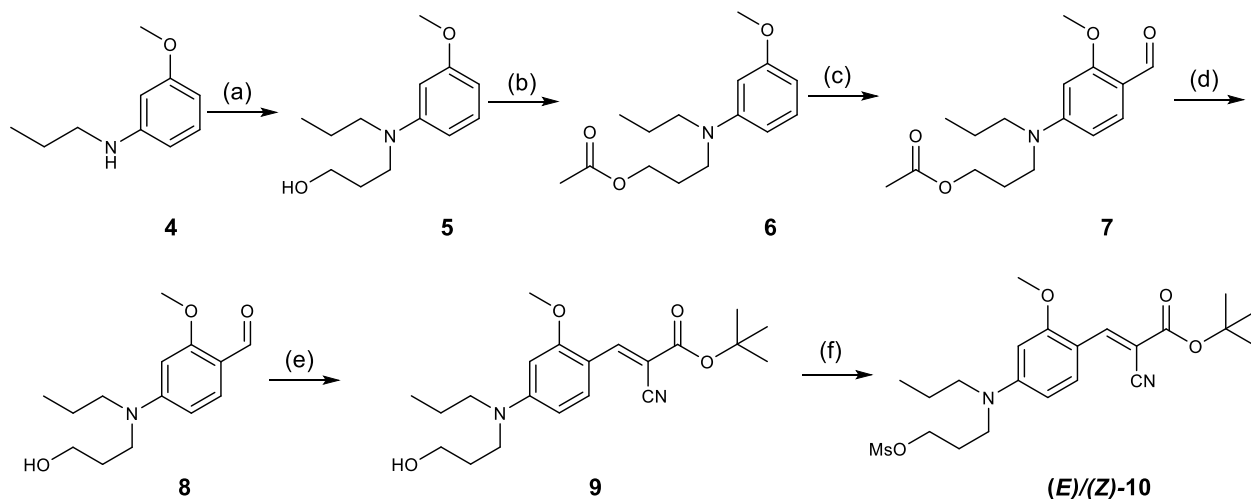

SCHEME 2 Synthesis of precursor **10**: a) Br(CH$_2$)$_3$OH, K$_2$CO$_3$, ACN, reflux, 88%; b) AcCl, pyridine, DCM, R.T.; c) POCl$_3$/DMF, 80 °C, 79%; d) K$_2$CO$_3$, MeOH/H$_2$O (1:1), 30 min, R.T.; e) *tert*-butyl cyanoacetate, piperidine, ACN, reflux, 90%; f) MsCl, Et$_3$N, DCM, 30 min, >98%

3.2 Radiochemistry

For the radiosynthesis of [^{18}F]**FACH**, a two-step approach including radiofluorination and deprotection was applied (Scheme 3). An alkali metal fluoride/cryptand complex such as K[^{18}F]F-K$_{2.2.2}$-carbonate is a reagent traditionally used for aliphatic nucleophilic substitution with ^{18}F-fluoride (24-28). This system is generally strongly basic, which restricts its synthetic utility for base-sensitive precursors because it generates various side reactions, such as eliminations of alkyl halides or sulfonates to form alkenes (29). On the other hand, tetraalkylammonium salts, such as Bu$_4$NHCO$_3$ (30), are milder reagents with enhanced solubility in organic solvents and have been

widely used as an alternative to the Kryptofix 2.2.2/K_2CO_3. In the current study, we investigated both agents for the radiosynthesis of [^{18}F]**FACH**.
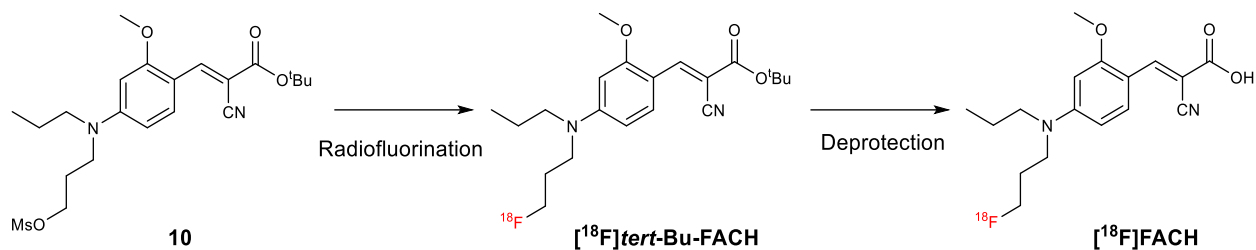
SCHEME 3 Two-step approach for the radiosynthesis of the novel MCT radioligand [^{18}F]**FACH**

3.2.1 Radiosynthesis of [^{18}F]FACH using K[^{18}F]F-K$_{2.2.2}$-carbonate complex

Optimization of the radiofluorionation via the K[^{18}F]F-K$_{2.2.2}$-carbonate system was accomplished by varying the amount of complex, solvent, reaction time and temperature. Attempts to obtain the intermediate [^{18}F]**tert-Bu-FACH** in a reasonable radiochemical yield (RCY) are summarized in Table 1. The radiofluorination was investigated in two solvents including DMSO and ACN using 11.2 mg (29.5 µmol) of K$_{2.2.2}$, 1.5 mg (10.5 µmol) of K_2CO_3 and aqueous solution of no-carrier-added [^{18}F]fluoride (hereinafter referred to as 100 mol% of K[^{18}F]F-K$_{2.2.2}$-carbonate complex) at a fixed concentration of the precursor **10** (2 mg, 4.4 µmol). In all cases, RCYs were higher in DMSO compared to ACN (Table 1).

Surprisingly, the amounts of K$_{2.2.2}$ and K_2CO_3 showed significant impact on the RCYs in both solvents based on the radio-HPLC analyses of the crude reaction mixture (Figure 3). While, only radiolabeled by-products were formed using 200 mol% of the K[^{18}F]F-K$_{2.2.2}$-carbonate complex in DMSO and ACN (Table 1, entries 1 and 4; Figure 3), by decreasing the complex amount to 100 mol%, [^{18}F]**tert-Bu-FACH** was detected in both solvent systems (Table 1, entries 2 and 5). Interestingly, further decrease of the basicity of the system (complex amount 50 mol%, entries 3 and 6, Table 1) promoted a substantial increase in the RCYs of [^{18}F]**tert-Bu-FACH** in both solvent systems investigated. However, the radiochemical yield was decreased when less than 50 mol% of the complex was used. In both solvents, the RCYs were diminished when the reactions were carried out at longer times or at higher temperatures (Table 1). Finally, the highest RCY for [^{18}F]**tert-Bu-FACH** was obtained using 50 mol% K[^{18}F]F-K$_{2.2.2}$-carbonate complex in DMSO at 100 °C in 20 min reaction time. Under this labeling condition, the ratio between *E*- and *Z*-isomers of [^{18}F]**tert-Bu-FACH** was found to be 99:1%.

FIGURE 3 Representative radio-HPLC chromatograms showing the effect of different amounts of the K[^{18}F]F-K$_{2.2.2}$-carbonate complex on the radiochemical yields of [^{18}F]**tert-Bu-FACH** in DMSO at 135 °C (left) and ACN at 100 °C (right); condition **A** was applied for HPLC measurements (see supplementary data)

The deprotection reaction was investigated using different concentrations of hydrochloric acid and trifluoroacetic acid (TFA) at different reaction times and temperatures (Table 2). The deprotection of [^{18}F]*tert*-**Bu-FACH** in DMSO by using both acids did not afford [^{18}F]**FACH** (Table 2, entries 1 and 2). Assuming that DMSO is not suitable as solvent for this conversion, we then performed the radiofluorination in ACN. The first attempts for removal of the *tert*-butyl group in ACN also failed, due to the conversion of [^{18}F]*tert*-**Bu-FACH** to radioactive by-products (Table 2, entries 3 and 4; Figure S5.1). This fact might be associated to (i) the thermal instability of [^{18}F]**FACH**, (ii) the remaining K[^{18}F]F-K$_{2.2.2}$-carbonate complex or (iii) the presence of water in the reaction mixture. Neither conducting the reaction at lower temperatures (at 40 °C or even at room temperature) nor removing the K[^{18}F]F-K$_{2.2.2}$-carbonate complex by using solid-phase extraction resulted in the formation of [^{18}F]**FACH**. However, the deprotection of [^{18}F]*tert*-**Bu-FACH** by using TFA in ACN under dry conditions afforded [^{18}F]**FACH** with RCY of 14.6 ± 6.4% (Table 2, entry 5). When dry dichloromethane (DCM) was used instead of ACN, [^{18}F]**FACH** was synthesized with RCYs of 26.7 ± 2.9% based on radio-HPLC of the crude reaction mixture (n = 3). Higher RCYs could be obtained at room temperature indicating that milder conditions prevent the formation of side products. However, subsequent attempts to neutralize the reaction mixture by using saturated Na$_2$CO$_3$ or 2.0 N NaOH revealed the decomposition of [^{18}F]**FACH** resulting in the same by-products as observed in our initial deprotection experiments (Figure S5.1), thus supporting the assumption of the impact of water on the stability of [^{18}F]**FACH** in the crude reaction mixture.

3.2.2 Radiosynthesis of [^{18}F]FACH using [^{18}F]TBAF

As an alternative radiosynthetic route for radiofluorination, tetra-n-butyl ammonium [^{18}F]fluoride ([^{18}F]TBAF) was used. First, the radiofluorination was investigated in a mixture of *tert*-BuOH and ACN (2:1) using 50 µl of tetra-n-butylammonium bicarbonate (0.075 M, aqueous solution) and an aqueous solution of no-carrier-added [^{18}F]fluoride at a fixed concentration of the precursor **10** (2 mg, 4.4 µmol) at different temperatures. In comparison to the radiofluorination using the K[^{18}F]F-K$_{2.2.2}$-carbonate system, RCYs of about 80% were obtained after 20 min at 100 °C as determined via radio-TLC and radio-HPLC analyses (Figure 4a, n = 3). Interestingly, the formation of *(Z)*-[^{18}F]*tert*-**Bu-FACH** was time- and temperature-dependent with the highest RCY of 27% at 110 °C after 20 min based on the radio-HPLC of the crude reaction mixture (Figures 4a-b). Nevertheless, the occurrence of the undesired *Z*-isomer did not diminish the formation of the final product, because after deprotection with TFA only the more stable *E*-isomer of [^{18}F]**FACH** could be detected, as confirmed by co-injection of the non-radioactive reference compound **FACH** (Figure S5.2). The deprotection of *(E)/(Z)*-[^{18}F]*tert*-**Bu-FACH** with TFA at room temperature afforded [^{18}F]**FACH** with RCYs of approximately 20%. Radio-HPLC analysis revealed an incomplete deprotection under these conditions as well as the formation of a new radioactive by-product, which might be a result of the presence of *tert*-BuOH in the crude mixture (Figure S5.2). Neither excess TFA nor longer reaction times promoted a complete deprotection of the intermediate [^{18}F]*tert*-**Bu-FACH**.

14

FIGURE 4 The effect of the reaction time and temperature on the radiochemical yields of *(E)-* and *(Z)*-[^{18}F]***tert*-Bu-FACH** in *tert*-BuOH/ACN (2:1): (a) the reaction was accomplished at 100 °C and samples were taken at different time points (b) the reactions were carried out at different temperatures for 20 min (n = 2)

Therefore, the possibility of implementing the radiofluorination in pure ACN was investigated. The radiofluorination in pure ACN rendered both isomers after 15 min at 100 °C with only slightly decreased RCYs [63.3 ± 10.8% and 7.6 ± 4.0% for *E*- and *Z*-isomers (n = 11, non-isolated), respectively], compared to *tert*-BuOH/ACN (2:1) [71.9 ± 13.2% and 4.6 ± 2.0% for *E*- and *Z*-isomers (n = 4, non-isolated), respectively]. Furthermore, no radioactive by-products were observed by deprotection of *(E)/(Z)*-[^{18}F]***tert*-Bu-FACH** with TFA in pure ACN at room temperature (Figure S5.3).

Upon completion of the reaction after 15 minutes, the excess TFA was neutralized with Et$_3$N. The radiotracer was isolated by semi-preparative RP-HPLC with 46% ACN/aq. 20 mM NH$_4$HCO$_2$, pH 4-5 as eluent (Figure 5a). [^{18}F]**FACH** was then purified, concentrated via solid-phase extraction and formulated in saline containing 10% (v/v) of EtOH for better solubility. Analytical radio-HPLC of the final product, co-eluted with the non-radioactive reference compound, confirmed the identity of the desired product (Figure 5b). At the end, [^{18}F]**FACH** was obtained with a RCY of 39.6 ± 8.3% (n = 10, end of bombardment), high radiochemical purity (>98%) and molar activities between 42-100 GBq/µmol (EOS), based on starting activities of 1-2 GBq.

FIGURE 5 (a) Representative semi-preparative radio- and UV-HPLC chromatograms of [^{18}F]**FACH** (conditions: Reprosil-Pur C18-AQ, 250 mm × 10 mm, 46% ACN/aq. 20 mM NH$_4$HCO$_2$, pH = 4-5, flow: 3.5 mL/min); (b) Representative analytical radio- and UV-HPLC chromatograms of [^{18}F]**FACH** co-eluted with the reference **FACH** (conditions: Reprosil-Pur C18-AQ, 250 mm × 4.6 mm, 46% ACN/aq. 20 mM NH$_4$HCO$_2$, pH = 4-5, flow: 1.0 mL/min)

3.2.3 The effect of pH on the deprotonation of [^{18}F]FACH

Interestingly, during further radio-HPLC experiments, two species of [^{18}F]**FACH** were observed which were corresponding to two species of the reference compound **FACH** observed under the same conditions (Figure 6). We therefore assumed that either deprotonation of the carboxylic acid group (Figure 6A) or photocatalytic *E* to *Z* isomerization (22) might be considered as possible mechanisms for the formation of these two forms. In order to investigate the hypothesis of an pH-dependent equilibrium between the two species of [^{18}F]**FACH**, a set of experiments was performed at which the pH value of the sample solutions was varied from 2.5-11.3. Only one HPLC signal was observed at pH values less than 5.5 which is probably related to the neutral form of [^{18}F]**FACH** (Figure 6B, left). When the pH values were higher than 6, a second HPLC signal at lower retention time was observed which can be designated to the deprotonated form of [^{18}F]**FACH** (Figure 6B, right; Figure S5.4). Based on these findings, the possibility of photocatalytic *E* to *Z* isomerization was investigated by exposing sample solutions of [^{18}F]**FACH** and **FACH** at pH value of 5 to

daylight. After a reasonable exposure time, the formation of a second species did not occur as proven by UV- and radio-HPLC analyses.

FIGURE 6 (A) Proposed pH-dependent equilibrium between neutral and deprotonated forms of [^{18}F]**FACH**; (B) Analytical radio- and UV-HPLC chromatograms represent two forms of [^{18}F]**FACH** at different pH (column: Reprosil-Pur C18-AQ, 250 × 4.6 mm, particle size: 5 µm; eluent: 46% ACN/aq. 20 mM NH_4HCO_2, pH = 4-5; flow: 1 mL/min).

4 CONCLUSIONS

The new fluorinated α-CHC derivative, **FACH**, showed high MCT1 and MCT4 inhibition comparable to the lead compound **I**, which made it suitable for the development of a novel ^{18}F-labeled radiotracer for PET imaging of MCTs. We herein investigated the use of the K[^{18}F]F-K$_{2.2.2}$-carbonate complex and [^{18}F]TBAF as phase transfer catalysts for radiosynthesis of the intermediate [^{18}F]*tert*-**Bu-FACH** and explored the influence of multiple reaction parameters to obtain [^{18}F]**FACH**. Our experiments revealed a base-sensitive behavior when using the conventional K[^{18}F]F-K$_{2.2.2}$-carbonate system as well as the formation of undesirable by-products during the deprotection step. By using the milder basic [^{18}F]TBAF system in ACN, the RCY of *(E)/(Z)*-[^{18}F]*tert*-**Bu-FACH** was nearly doubled in comparison to the K[^{18}F]F-K$_{2.2.2}$-carbonate system. Moreover, [^{18}F]TBAF offered a relevant route for the radiosynthesis of [^{18}F]**FACH** via a two-step one-pot strategy. [^{18}F]**FACH** was finally obtained in high radiochemical yield and purity within a reliable and reproducible radiosynthesis route, which is intended to be translated to an automated module device for large-scale production of the radiotracer. This newly developed radiotracer is expected to enable PET investigations of solid tumors expressing MCTs.

REFERENCES

1. Halestrap AP, Meredith D. The SLC16 gene family-from monocarboxylate transporters (MCTs) to aromatic amino acid transporters and beyond. *Pflügers Archiv* 2004;447(5):619-628.

2. Bröer S, Schneider H-P, Bröer A, Rahman B, Hamprecht B, Deitmer JW. Characterization of the monocarboxylate transporter 1 expressed in Xenopus laevis oocytes by changes in cytosolic pH. *Biochem J* 1998;333(1):167-174.

3. Dimmer K-S, Friedrich B, Florian L, Deitmer JW, Bröer S. The low-affinity monocarboxylate transporter MCT4 is adapted to the export of lactate in highly glycolytic cells. *Biochem J* 2000;350(1):219-227.

4. Fox JEM, Meredith D, Halestrap AP. Characterisation of human monocarboxylate transporter 4 substantiates its role in lactic acid efflux from skeletal muscle. *J Physiol* 2000;529(2):285-293.

5. Ponizovskiy MR. Warburg effect mechanism as the target for theoretical substantiation of new possibility cancer disease treatment. *Crit Rev Eukaryot Gene Expr* 2011;21(1):13-28.

6. Koppenol WH, Bounds PL, Dang CV. Otto Warburg's contributions to current concepts of cancer metabolism. *Nat Rev Cancer* 2011;11(5):325-337.

7. Gurrapu S, Jonnalagadda SK, Alam MA, Nelson GL, Sneve MG, Drewes LR, et al. Monocarboxylate transporter 1 inhibitors as potential anticancer agents. *ACS Med Chem Lett* 2015;6(5):558-561.

8. Mereddy VR, Drewes LR, Alam MA, Jonnalagadda SK, Gurrapu S. Therapeutic compounds. Google Patents; 2016, US 9,296,728 B2.

9. Doherty JR, Yang C, Scott KE, Cameron MD, Fallahi M, Li W, et al. Blocking lactate export by inhibiting the Myc target MCT1 Disables glycolysis and glutathione synthesis. *Cancer Res* 2013;74(3):908-920.

10. Fang J, Quinones QJ, Holman TL, Morowitz MJ, Wang Q, Zhao H, et al. The H^+-linked monocarboxylate transporter (MCT1/SLC16A1): a potential therapeutic target for high-risk neuroblastoma. *Mol Pharmacol* 2006;70(6):2108-2115.

11. Sanità P, Capulli M, Teti A, Galatioto GP, Vicentini C, Chiarugi P, et al. Tumor-stroma metabolic relationship based on lactate shuttle can sustain prostate cancer progression. *BMC Cancer* 2014;14(1):154-167.

12. Baek G, Tse Yan F, Hu Z, Cox D, Buboltz N, McCue P, et al. MCT4 Defines a Glycolytic Subtype of Pancreatic Cancer with Poor Prognosis and Unique Metabolic Dependencies. *Cell Rep* 2014;9(6):2233-2249.

13. Curry JM, Tuluc M, Whitaker-Menezes D, Ames JA, Anantharaman A, Butera A, et al. Cancer metabolism, stemness and tumor recurrence: MCT1 and MCT4 are functional biomarkers of metabolic symbiosis in head and neck cancer. *Cell Cycle* 2013;12(9):1371-1384.

14. Cairns RA, Harris IS, Mak TW. Regulation of cancer cell metabolism. *Nat Rev Cancer* 2011;11(2):85-95.

15. Poole RC, Halestrap AP. Transport of lactate and other monocarboxylates across mammalian plasma membranes. *Am J Physiol-Cell Physiology* 1993;264(4):C761-C782.

16. Meredith D, Christian H. The SLC16 monocaboxylate transporter family. *Xenobiotica* 2008;38(7-8):1072-1106.

17. Murray CM, Hutchinson R, Bantick JR, Belfield GP, Benjamin AD, Brazma D, et al. Monocarboxylate transporter MCT1 is a target for immunosuppression. *Nat Chem Biol* 2005;1(7):371-376.

18. https://clinicaltrials.gov/ct2/show/NCT01791595.

19. Wang X, Levi A, Halestrap A. Substrate and inhibitor specificities of the monocarboxylate transporters of single rat heart cells. *Am J Physiol Heart and Circulatory Physiology* 1996;270(2):H476-H484.

20. Graham K, Müller A, Lehmann L, Koglin N, Dinkelborg L, Siebeneicher H. [^{18}F] Fluoropyruvate: radiosynthesis and initial biological evaluation. *J Label Compd Radiopharm* 2014;57(3):164-71.

21. Van Hée VF, Labar D, Dehon G, Grasso D, Grégoire V, Muccioli GG, et al. Radiosynthesis and validation of (±)-[^{18}F]-3-fluoro-2-hydroxypropionate ([^{18}F]-FLac) as a PET tracer of lactate to monitor MCT1-dependent lactate uptake in tumors. *Oncotarget* 2017;8(15):24415-24428.

22. Tateishi H, Tsuji AB, Kato K, Sudo H, Sugyo A, Hanakawa T, et al. Synthesis and evaluation of ^{11}C-labeled coumarin analog as an imaging probe for detecting monocarboxylate transporters expression. *Bioorg Med Chem Lett* 2017;27(21):4893-4897.

23. Vilsmeier A, Haack A. Über die Einwirkung von Halogenphosphor auf Alkyl-formanilide. Eine neue Methode zur Darstellung sekundärer und tertiärer p-Alkylamino-benzaldehyde. *Eur J Inorg Chem* 1927;60(1):119-122.

24. Gokel GW. Crown ethers and cryptands: monographs in supramolecular chemistry. Edited by: Stoddart, JF. London: Royal Society of Chemistry. 1991. 190 p.

25. Dehmlow EV, Dehmlow SS. Phase transfer catalysis. Weinheim; Wiley-VCH. 1993. 499 p.

26. Jacobson O, Kiesewetter DO, Chen X. Fluorine-18 radiochemistry, labeling strategies and synthetic routes. *Bioconjugate Chem* 2014;26(1):1-18.

27. Li S, Schmitz A, Lee H, Mach RH. Automation of the radiosynthesis of six different ^{18}F-labeled radiotracers on the AllinOne. *EJNMMI Radiopharm Chem* 2017;1(1):15-33.

28. Wiemer J, Steinbach J, Pietzsch J, Mamat C. Preparation of a novel radiotracer targeting the EphB4 receptor via radiofluorination using spiro azetidinium salts as precursor. *J Label Compd Radiopharm* 2017;60(10):489-498.

29. Pilcher AS, Ammon HL, DeShong P. Utilization of tetrabutylammonium triphenylsilyldifluoride as a fluoride source for nucleophilic fluorination. *J Am Chem Soc* 1995;117(18):5166-5167.

30. Cox DP, Terpinski J, Lawrynowicz W. " Anhydrous" tetrabutylammonium fluoride: a mild but highly efficient source of nucleophilic fluoride ion. *J Org Chem* 1984;49(17):3216-3219.

TABLE 1 Investigated parameters for radiosynthesis of [^{18}F]*tert*-**Bu-FACH**[a]

Entry	Solvent	K[^{18}F]F-K$_{2.2.2}$-carbonate complex (mol%)	Temp. (°C)	Time (min)	Radiochemical yield (%)[b]
1	DMSO	200	110, 130, 150	10, 20, 30	0
2	DMSO	100[c]	110, 120, 135	10, 20, 30	22.3 ± 5.5
3	**DMSO**	**50**	**135**	**20**	**45.0 ± 9.5**
4	ACN	200	90, 100, 110	5, 10, 15, 20	0
5	ACN	100	90, 100, 110	5, 10, 15, 20	19.7 ± 2.1
6	**ACN**	**50**	**100**	10, **15**, 20	**38.7 ± 14.9**

[a] In all experiments, 2 mg (4.4 µmol) of precursor **10** was used in a total reaction volume of 750 µl; [b] The RCYs were determined based on the radio-HPLC analysis of the crude reaction mixture (n ≥ 3, non-isolated); [c] 100 mol% of K[^{18}F]F-K$_{2.2.2}$-carbonate complex represents 11.2 mg (29.5 µmol) of Kryptofix 2.2.2 and 1.5 mg (10.5 µmol) of K$_2$CO$_3$.

TABLE 2 Investigated parameters for the formation of [^{18}F]**FACH**

Entry	Solvent	Acid	Temp. (°C)	Time (min)	Radiochemical yield (%)[a]
1	DMSO	HCl (2,6 N)	85, 100, 115	5, 10, 15, 20	0
2	DMSO	TFA	85	10, 20	0
3	ACN	HCl (2,6 N)	r.t., 40, 85	5, 10	0
4	ACN	TFA/H$_2$O	r.t., 40, 85	10, 15, 20	0
5	ACN	TFA	r.t., 40, 85	10, 15, 20	14.6 ± 6.4[b]
6	**DCM**	**TFA**	**r.t.**, 40	10, **15**, 20	**26.7 ± 2.9**[b]

[a] The radiochemical yields were determined based on radio-TLC and radio-HPLC analyses of the crude reaction mixture (n ≥ 3, non-isolated); [b] Evaporation of TFA was needed before separation.